

# Photoemission spectra of a two-dimensional $S = 1/2$ quantum antiferromagnet in magnetic fields: a theoretical study

Wei-Guo Yin and W. N. Mei

Department of Physics, University of Nebraska, Omaha, NE 68182

(Dated: April 14, 2024)

We calculate the angular resolved photoemission spectra (ARPES) of a spin-1/2 Heisenberg antiferromagnet as a function of magnetic fields using both the exact diagonalization method and self-consistent Born approximation. Below the saturation field  $B_C$ , strong scattering between spin waves and a hole, created by photoemission of an electron, significantly narrows the quasiparticle band that is characterized by the lowering of the quasiparticle energy at  $(\pi, \pi)$  with increasing field. Accordingly, in ARPES the quasiparticle peak gets sharper near  $(\pi, \pi)$  and broader elsewhere. Furthermore, we observe that an anomalous extended van Hove region (EVHR) around  $(\pi, \pi)$  appears in a half saturation field, while EVHRs around  $(\pi, 0)$  and  $(0, \pi)$  in zero field gradually disappear with increasing field.

PACS numbers: 75.50.Ee, 75.40.Gb, 79.60.-i

The effect of a strong magnetic field on quantum spin systems has played an integral role in the understanding of magnetism and quantum phase transitions. There is renewed interest in this topic due to the synthesis of a new family of low-dimensional quantum antiferromagnets with small exchange constants [1, 2, 3, 4]. For example, the theoretical prediction of field-induced incommensurate soft modes in one-dimensional (1D) spin-1/2 quantum antiferromagnet (AFM) was confirmed by neutron scattering experiments on copper benzoate [1], while anomalous spin excitation spectrum of a 2D AFM in strong fields has been reported [5, 6]. Other important observations include superconductivity in a layered organic AFM at very high magnetic fields [7, 8]. In this paper, we present a theoretical study of the magnetic field dependence of the angular resolved photoemission spectra (ARPES) in a 2D AFM.

Zero-field ARPES experiments in a 2D AFM are important to the research of many cuprate superconductors whose undoped parent compounds are nearly square lattice spin-1/2 antiferromagnetic insulators [9]. It was revealed that the presence of strong scattering processes between spin waves and a hole, created by emission of an electron, gives rise to an extended van Hove singularity near the Fermi surface. This novel feature is crucial in understanding many other anomalous physical properties of the cuprate superconductors and could be explained in the spin-polaron picture [10, 11]. On the other hand, above the critical field  $B_C$ , the system becomes a saturated ferromagnet and the ARPES are known to be free-particle like. Therefore, it would be interesting to study the evolution of the ARPES of a 2D AFM from one limit to the other, in particular, the change of the extended van Hove regions. To our knowledge, this problem remains unanswered, primarily because the exchange constants in typical planar cuprates are  $J \approx 1500$  K, hence, only near zero-field studies were possible. Nevertheless, a newly fabricated family of spin-1/2 square lattice antiferromagnets,

(5CAP) $_2$ CuX $_4$  and (5MAP) $_2$ CuX $_4$  with X = Cl or Br [2, 3, 4], was found to have small  $J' \approx 0.57 \pm 0.5$  K with  $B_C \approx 24$  T, thus provides a good testing ground for our theoretical analysis. Alternatively, the ARPES studies could be carried out in certain pseudospin systems where the effective magnetic field  $B_e$  is comparable with the effective exchange constant  $J_e$ ; for instance, in a mixed valence system with electronic ferroelectricity [12, 13],  $B_e$  is the d- and f-level energy difference that could be as large as  $J_e$  and adjustable by alloying or applying pressure. In the present work, we observe a magnetic-field-induced anomalous  $\pi$  region around  $(\pi, \pi)$ , where the bottom of the quasiparticle band locates, in a magnetic field of  $\frac{1}{2}B_C$ , signifying an extended van Hove singularity near the Fermi surface from zero field up to  $\frac{1}{2}B_C$ .

Our starting point is a 2D t-J model, a simple yet effective Hamiltonian to model layered cuprate superconductors, in a magnetic field along z direction,

$$H = \sum_{\langle i,j \rangle} t \sum_{\sigma} (c_i^{\sigma} c_j^{\sigma} + c_j^{\sigma} c_i^{\sigma}) + J \sum_{\langle i,j \rangle} \tilde{c}_i^{\dagger} \tilde{c}_j^{\dagger} B_i^z; \quad (1)$$

where  $\tilde{c}_i = c_i (1 - n_{i\uparrow})$  is the constrained fermion operator, and  $\tilde{c}_i^{\dagger} = c_i^{\dagger} (1 - n_{i\downarrow})$  with  $f = \uparrow, \downarrow$  being the Pauli matrices is the spin operator. The SU(2) symmetry is broken in the presence of an applied magnetic field, for the AFM will orient itself in such a way that the staggered direction, which is chosen to be the x direction, is perpendicular to the applied field. The resulting magnetic phase is a canted state of two sublattices in which the spins tilt towards the z axis by the angle  $\theta = \arccos(B/B_C)$  with the saturation field  $B_C = 4J$ . Note that  $\theta = 0$  for  $B = B_C$ . The Hamiltonian is invariant under rotation of spins around the z axis, hence the spin excitation spectrum should be a gapless Goldstone mode.

The ARPES are defined as

$$A(k;!) = \sum_{j,l} \langle j_l | v_j | j_l \rangle \langle j_l | j_l \rangle^2 (E_0 + E_{1,l}); \quad (2)$$

where  $E_0$  and  $j_l$  are the ground-state energy and eigenvector without any hole, and  $E_{1,l}$  and  $j_l$  are the energy and the wave vector of the  $l$ -th eigenstate with one hole created by photoemission of one electron. To calculate  $A(k;!)$ , we first employ the Lanczos exact diagonalization (ED) algorithm [14] with 100 iterations and an artificial broadening factor  $\gamma = 0.05t$  on a  $4 \times 4$  square cluster. Furthermore, in order to overcome the finite size effect in the ED calculations and gain more insights, we perform in the following analytical calculations of  $A(k;!)$  in the spin-polaron picture in the context of the self-consistent Born approximation.

To simplify the notation, it is convenient to perform a rotation of the spins in the A and B sublattices by  $\pi$  and about the  $y$  axis, respectively:

$$\begin{aligned} e_{1*} &= \cos \frac{\alpha}{2} d_{1*} - e^{iQ} \sin \frac{\alpha}{2} d_{1\#}; \\ e_{1\#} &= e^{iQ} \sin \frac{\alpha}{2} d_{1*} + \cos \frac{\alpha}{2} d_{1\#}; \\ S_i^x &= S_i^x \cos \frac{\alpha}{2} + S_i^z e^{iQ} \sin \frac{\alpha}{2}; \\ S_i^z &= S_i^z \cos \frac{\alpha}{2} - S_i^x e^{iQ} \sin \frac{\alpha}{2}; \end{aligned}$$

where  $\frac{\alpha}{2} = S_i^y$  and  $Q = \frac{\alpha}{2}$ .  $d_i$  are constrained fermion operators and  $S_i = \frac{1}{2} d_i^\dagger \sim d_i$  are spin operators in the new local coordinate system. This canonical transformation maps the canted spin configuration to a ferromagnetic configuration with all spins up and removes further necessity to distinguish between sublattices. The Hamiltonian thus has the form  $H = H_t + H_J$ , where

$$H_t = -t \cos \frac{\alpha}{2} \sum_{i,j} (d_{i*}^\dagger d_{j*} + d_{i\#}^\dagger d_{j\#}) - t \sin \frac{\alpha}{2} \sum_{i,j} e^{iQ} (d_{i*}^\dagger d_{j\#} + d_{i\#}^\dagger d_{j*}) + H_{\text{sc}}; \quad (3)$$

$$\begin{aligned} H_J &= J \sum_{i,j} (S_i^z S_j^z \cos 2\frac{\alpha}{2} + S_i^x S_j^x \cos 2\frac{\alpha}{2} + S_i^y S_j^y) \\ &+ J \sin 2\frac{\alpha}{2} \sum_{i,j} (S_i^z S_j^x - S_i^x S_j^z) \\ &+ B \sin \frac{\alpha}{2} \sum_i S_i^x e^{iQ} - B \cos \frac{\alpha}{2} \sum_i S_i^z; \quad (4) \end{aligned}$$

Then, we treat quantum spin fluctuations within linear spin wave theory [13, 15], namely, we regard the deviations of the spins measured from their equilibrium directions are small, hence only up to the quadratic terms of the deviation operators are retained in  $H_J$ . Since the equilibrium directions are determined from vanishing of the linear terms, the second and third terms

in  $H_J$  that are linear in spin deviations could be neglected. Note that there are spin-flipping hopping terms  $\propto e^{iQ} (d_{i*}^\dagger d_{j\#} - d_{i\#}^\dagger d_{j*})$  in  $H_t$ , which represent emitting and absorbing spin excitations, thus contribute to strong scattering processes between the hole and spin waves. Taking the ferromagnetic configuration as the vacuum state, we employ the slave-fermion formalism to cope with the constraint of no doubly occupancy in  $H_t$  [16]. Defining holon (spinless fermion) operators  $h_i$  so that  $d_{i*} = h_i^\dagger$ ,  $d_{i\#} = h_i^\dagger a_i$  where  $a_i = S_i^+$  is the hard-core boson operator, we arrive at an effective spin-polaron Hamiltonian in the momentum space

$$H = \sum_k \epsilon_k h_k^\dagger h_k + \sum_q \epsilon_q a_q^\dagger a_q + \sum_{k,q} M_{kq} h_k^\dagger h_{k-q} + H_{\text{sc}}; \quad (5)$$

where  $a_q$ 's are spin wave operators,  $a_q = u_q a_q + v_q a_{-q}^\dagger$ , with dispersion  $\epsilon_q = (A_q^2 - B_q^2)^{1/2}$ . The transformation coefficients are  $u_q = [(A_q - \epsilon_q)/2]^{1/2}$  and  $v_q = [\text{sgn}(B_q) (A_q + \epsilon_q)/2]^{1/2}$ . Here the shorthand notations are  $A_q = 2J(1 + \cos^2 q)$ ,  $B_q = 2J \sin^2 q$ , and  $q = (\cos q_x a + \cos q_y a)/2$  with the lattice constant  $a$  being the length unit in the following. Note that the spin-wave spectrum is indeed gapless ( $\epsilon_{q=Q} = 0$ ). The bare hole dispersion is  $\epsilon_k = 4t \cos k$ , and the hole-spin-wave coupling is

$$M_{kq} = \sin \frac{q}{N} (\epsilon_k u_{q+Q} + \epsilon_{k-Q} v_{q+Q}); \quad (6)$$

Using the self-consistent Born approximation (SCBA) in which the spectral functions of one hole in a  $t$ - $J$ -like model can be accurately calculated [11, 16, 17, 18, 19], that is, we first compute the hole Green's function  $G(k;!) = [\epsilon_k - \epsilon(k;!) + i0^+]^{-1}$  self-consistently with the self-energy,

$$\Sigma(k;!) = \sum_q M_{kq}^2 G(k-q;!) \epsilon_{q+Q}; \quad (7)$$

Thus, the spectral functions of the hole quasiparticle (QP) are given by  $A(k;!) = -\text{Im} G(k;!)$ , the spectral weights are  $Z(k) = [1 - \partial \epsilon(k;!) / \partial \epsilon_k]_{\epsilon=E_k}^{-1}$ , and the QP dispersion is  $E_k = \epsilon_k + \text{Re} \Sigma(k;E_k)$ .

To examine the finite size effect, we start the SCBA calculations with a  $4 \times 4$  square lattice and compare the results with those obtained from using ED, then gradually increase the lattice size. Finally, we find that the SCBA results obtained from a  $32 \times 32$  lattice are rather close (within 1%) to those from a  $16 \times 16$  lattice. This implies that the SCBA results on the  $16 \times 16$  lattice are not seriously affected by the boundary effect. Since in typical cuprates,  $J = 0.2 - 0.5t$ , we will adopt  $J = 0.4t$  in our calculations. The energy mesh is chosen from  $-6t$  to  $6t$  with interval  $0.01t$ .

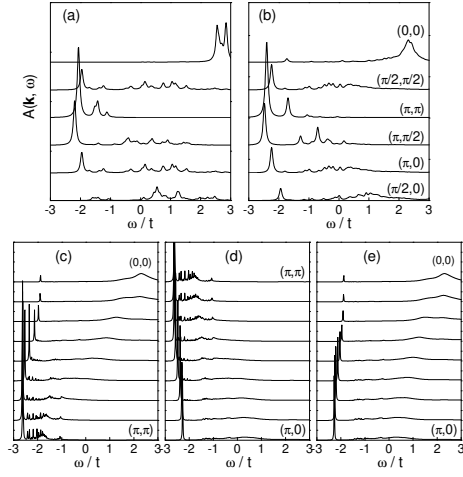


FIG. 1: The ARPES  $A(k; \omega)$  of the  $4 \times 4$  antiferromagnet for  $J = 0.4t$  and  $B = \frac{1}{2}B_c$  using (a) ED and (b) SCBA. (c)–(e) present the ARPES of the  $16 \times 16$  antiferromagnet along (c)  $(0;0)$  ( $\pi; \pi$ ), (d)  $(\pi; \pi)$  ( $\pi; 0$ ) and (e)  $(\pi; 0)$  ( $0;0$ ) directions using SCBA.

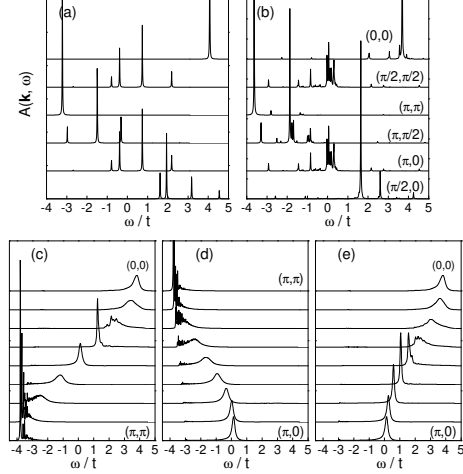


FIG. 2: Same as in Fig. 1, except for  $B = \frac{7}{8}B_c$ .

Then we proceed to compare the ED and SCBA results. From the ARPES  $A(k; \omega)$  of the  $4 \times 4$  AFM in Figs. 1(a)–(b) for  $B = \frac{1}{2}B_c$  and in Figs. 2(a)–(b) for  $B = \frac{7}{8}B_c$ , we notice that the line shapes obtained from using ED [Figs. 1(a) and 2(a)] agree well with those obtained from SCBA [Figs. 1(b) and 2(b)]. As for the results for  $B = 0$ , we refer readers to Ref. [14, 17]. These numerics unambiguously demonstrate that the spin-polaron picture provides indeed a natural description of the QP behavior. In addition, the ARPES of the  $16 \times 16$  AFM obtained from using SCBA shown in Figs. 1(c)–(e) and Fig. 2(c)–(e) are in consistency with those obtained from the  $4 \times 4$  AFM. The main feature of these ARPES is that as  $B$  increases, the spectrum at  $(\pi; \pi)$ , the QP band bottom, gets more and more coherent, while away from the band bottom the spectra be-

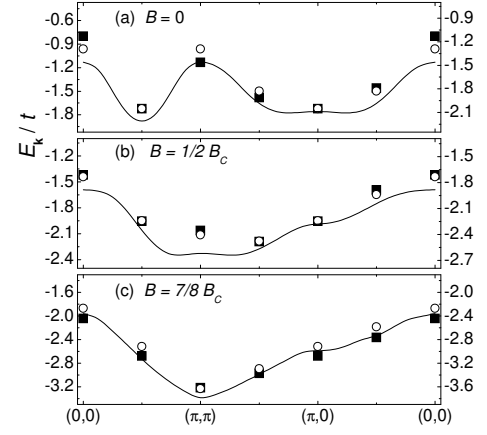


FIG. 3: Quasiparticle dispersion for  $J = 0.4t$  and  $B = 0$  (a),  $\frac{1}{2}B_c$  (b), and  $\frac{7}{8}B_c$  (c). Left label: ED results (solid squares) on the  $4 \times 4$  square lattice. Right label: SCBA on the  $4 \times 4$  (open circles) and  $16 \times 16$  (solid lines) lattices.

comes incoherent quickly, indicating that the QP states away from the minimum decay by emission of spin waves.

Furthermore, we present in Fig. 3 the calculated electronic structure of the 2D Heisenberg AFM with  $B = 0$ ,  $\frac{1}{2}B_c$  and  $\frac{7}{8}B_c$ , respectively. Again, the SCBA results agree well with those obtained from ED. We notice three main features in these quasiparticle bands: First, as  $B$  increases, the band bottom evolves from  $(\pi; \pi)$  to  $(\pi; 0)$ . Second, the low-energy band [Fig. 3(a)] has flat regions around  $(\pi; 0)$  and  $(0; \pi)$ , while the high-energy band [Fig. 3(c)] resembles the free particle dispersion but its width is severely narrowed. In between, for  $B = \frac{1}{2}B_c$  [Fig. 3(b)], a new anomalous feature, a flat region around  $(\pi; \pi)$ , appears in the electronic structure, which leads to a strongly distorted density of states with a massive peak near the bottom of the QP band. Therefore, an extended van Hove singularity near the bottom of the QP band survives up to  $B = \frac{1}{2}B_c$ . Third, the QP bandwidth is strikingly narrowed, which can be seen more clearly in Table I.

In Table I, we present several interesting physical quantities, including the QP bandwidth  $W$ , the spin-wave bandwidth  $W_{sw}$ , the minimum QP energy  $E_{min}$ , and the QP spectral weights  $Z(k)$  at high symmetric points in the first Brillouin zone, as a function of the magnetic field. These data are obtained from using SCBA on the  $16 \times 16$  lattice. We find that  $W$  and  $W_{sw}$  have similar values. Such band narrowing can be understood as follows: since gapless spin excitations are easily stimulated by the incoherent motion of a hole, the combination of the hole and polarized spin-wave cloud constitutes the quasiparticle, spin-polaron. Hence,  $W$  scales with  $W_{sw}$ . Another special feature revealed from Table I is that in low fields the largest spectral weights locate at  $(\pi; \pi)$  and  $(\pi; 0)$ ; increasing  $B$  would raise  $Z(\pi; \pi)$ , while it decreases the QP spectral weights at other wave vectors.

TABLE I:  $E_{\text{min}}$ , the minimal QP energy,  $W$ , the QP bandwidth,  $W_{\text{sw}}$ , the spin-wave bandwidth, and  $Z(\mathbf{k})$ , the QP spectral weights at several high symmetric points in the first Brillouin zone as a function of  $B$ , the magnetic field, obtained on the  $16 \times 16$  lattice using SCBA for  $J = 0.4t$ .

$B/B_C$	$E_{\text{min}}/t$	$W/t$	$W_{\text{sw}}/t$	$Z(0;0)$	$Z(\frac{\pi}{2};\frac{\pi}{2})$	$Z(\frac{\pi}{2};0)$	$Z(0;\frac{\pi}{2})$
0	-2.209	0.748	0.800	0.1112	0.3466	0.1112	0.3821
1/8	-2.213	0.731	0.800	0.0580	0.3426	0.2047	0.3730
2/8	-2.269	0.685	0.801	0.0406	0.3147	0.3068	0.3431
3/8	-2.399	0.674	0.811	0.0304	0.2587	0.3946	0.2907
4/8	-2.639	0.757	0.849	0.0214	0.1809	0.4698	0.2178
5/8	-3.021	0.972	1.000	0.0121	0.0857	0.5300	0.1298
6/8	-3.418	1.199	1.200	0.0076	0.0186	0.5891	0.0447
7/8	-3.786	1.427	1.400	0.0013	0.0013	0.6550	0.0043
1	-4	8	1.600	1	1	1	1

This confirms the spectral features shown in Figs. 1 and 2. We explain this feature as follows: in low fields the spins are almost antiferromagnetically aligned, therefore the effective hole hopping in the same sublattice would be favored, leading to  $E_{\text{min}}$  at  $(\pi, \pi)$  and considerably large values of  $Z(\pi, \pi)$  and  $Z(\pi, 0)$ . On the contrary, increasing  $B$  will raise the bare hole dispersion  $\epsilon_{\mathbf{k}}/\cos \theta = B/B_C$  and decrease the hole-spin-wave coupling  $M_{\mathbf{k}q}/\sin \theta$ , thus facilitates the hole propagation to nearest neighboring sites and lowers the QP energy at  $\mathbf{k} = (\pi, 0)$ , whereas hole motion with other wave vectors is impeded due to scattering of spin waves. We notice from Table I that  $W$  and  $Z(\mathbf{k})$  experience abrupt change as  $B \rightarrow B_C$ . In this limit, Eq. (7) can be solved analytically in perturbation theory, since  $M_{\mathbf{k}q} \rightarrow 0$  as  $B \rightarrow B_C$ . Hence, the QP dispersion is given by

$$E_{\mathbf{k}} = \epsilon_{\mathbf{k}} + \sum_q \frac{M_{\mathbf{k}q}^2}{\epsilon_{\mathbf{k}} - \epsilon_{\mathbf{k}+q}} = \epsilon_{\mathbf{k}} + O(1/B_C): \quad (8)$$

Above  $B_C$ ,  $M_{\mathbf{k}q} = 0$ , thus  $E_{\mathbf{k}} = \epsilon_{\mathbf{k}} = 4t_{\mathbf{k}}$ , that is, the hole moves freely in a saturated ferromagnet.

It is worth mentioning that linear spin-wave theory was pointed out to be inaccurate in strong fields (spin waves in a quantum AFM in a strong field  $> 0.76B_C$ ) were unstable with respect to the spontaneous two-magnon decays [6]. Nevertheless, we have demonstrated that the strong-field ARPES obtained from using the SCBA, where the spin excitations are treated in linear spin-wave theory, agree well with the ED results. Hence, it appears that linear spin-wave theory is appropriate to calculate the spectral functions of a hole in a quantum AFM. While it is desirable to follow the present study with high order spin-wave theory or ED for larger lattices, we anticipate that our basic conclusions remain valid.

To summarize, we have studied the magnetic field dependence of the ARPES of a square lattice spin-1/2

Heisenberg antiferromagnet. Using the self-consistent Born approximation in the spin-polaron picture, we observe an anomalous electronic structure in which an extended van Hove region around  $(\pi, 0)$  in zero field moves toward  $(\pi, \pi)$  with increasing field strength until reaching a half saturation field. We also present the exact diagonalization data that confirm our prediction, which could be tested by ARPES experiments on weakly interacting spin-1/2 square lattice antiferromagnets [2, 3, 4].

We are grateful to C. D. Batista and H.-Q. Lin for useful discussions. This work was supported by the Nebraska EPSCoR NSF Grant EPS-9720643 and the Office of Naval Research.

Electronic address: wgyin@yahoo.com

- [1] D. C. Dender, P. R. Hammar, D. H. Reich, C. Broholm, and G. Aeppli, Phys. Rev. Lett. 79, 1750 (1997).
- [2] P. Zhou, J. E. Drumheller, G. V. Rubenacker, K. Halvorsen, and R. D. Willett, J. Appl. Phys. 69, 5804 (1991).
- [3] P. R. Hammar, D. C. Dender, and D. H. Reich, J. Appl. Phys. 81, 4615 (1997).
- [4] F. M. Woodward, A. S. Albrecht, C. M. Wynn, and C. P. Landee, Phys. Rev. B 65, 144412 (2002).
- [5] O. F. Syljuasen and P. A. Lee, Phys. Rev. Lett. 88, 207207 (2002).
- [6] M. E. Zhitomirsky and A. L. Chemsyhev, Phys. Rev. Lett. 82, 4536 (1999).
- [7] S. Uji, H. Shinagawa, T. Terashima, T. Yakabe, Y. Terai, M. Tokumoto, A. Kobayashi, H. Tanaka, and H. Kobayashi, Nature (London) 410, 908 (2001).
- [8] L. Balicas, J. S. Brooks, K. Storr, S. Uji, M. Tokumoto, H. Tanaka, H. Kobayashi, A. Kobayashi, V. Barzykin, and L. P. Gor'kov, Phys. Rev. Lett. 87, 067002 (2001).
- [9] A. Damascelli, Z.-X. Shen, and Z. Hussain, Rev. Mod. Phys. 75, 473 (2003).
- [10] C. Kim, P. J. White, Z.-X. Shen, T. Tohyama, Y. Shiba, S. Maekawa, B. O. Wells, Y. J. Kim, R. J. Birgeneau, and M. A. Kastner, Phys. Rev. Lett. 80, 4245 (1998).
- [11] W.-G. Yin, C. D. Gong, and P. W. Leung, Phys. Rev. Lett. 81, 2534 (1998).
- [12] C. D. Batista, Phys. Rev. Lett. 89, 166403 (2002).
- [13] W.-G. Yin, W. N. Mei, C.-G. Duan, H.-Q. Lin, and J. Hardy, cond-mat/0302554.
- [14] E. Dagotto, Rev. Mod. Phys. 66, 763 (1994).
- [15] M. E. Zhitomirsky and T. Nikuni, Phys. Rev. B 57, 5013 (1998).
- [16] S. Schmitt-Rink, C. M. Varma, and A. E. Ruckenstein, Phys. Rev. Lett. 60, 2793 (1988).
- [17] P. W. Leung and R. J. Gooding, Phys. Rev. B 52, 15711 (1995).
- [18] J. Bala, A. M. Oles, and J. Zaanen, Phys. Rev. B 52, 4597 (1995).
- [19] W.-G. Yin, H. Q. Lin, and C. D. Gong, Phys. Rev. Lett. 87, 047204 (2001).